Virology 275, 158–169 (2000)
doi:10.1006/viro.2000.0477, available online at http://www.idealibrary.com on IDEAL®



# Heteroclite Subgenomic RNAs Are Produced in Porcine Reproductive and Respiratory Syndrome Virus Infection

Shishan Yuan, Michael P. Murtaugh, and Kay S. Faaberg[1]

*Department of Veterinary PathoBiology, College of Veterinary Medicine, University of Minnesota, 1971 Commonwealth Avenue, St. Paul, Minnesota 55108*

*Received April 18, 2000; returned to author for revision May 31, 2000; accepted June 19, 2000*

Porcine reproductive and respiratory syndrome virus (PRRSV) was shown to produce atypical subgenomic RNAs that contain open reading frame 1a nucleotides and are present under a wide variety of culture conditions, including high and low multiplicities of infection, in simian and porcine host cells, and during infection with cell-adapted and wild-type PRRSV strains. Sequence analysis demonstrated that they are heterogeneous in 5′–3′ junction sequence and size and may code for different predicted fusion proteins. This is the first report of these novel RNAs in arteriviruses and we have termed them heteroclite (meaning "deviating from common forms or rules") subgenomic RNAs. The unique properties of these subgenomic RNAs include (a) apparent association with normal virus infection and stability during serial passage, (b) packaging of heteroclite RNAs into virus-like particles, (c) short, heterogeneous sequences which may mediate the generation of these RNAs, (d) a primary structure which consists of the two genomic termini with one large internal deletion, and (e) little apparent interference with parental virus replication. These subgenomic RNAs may be critical to, or a necessary side product of, viral replication. The expression of these novel RNA species support the template-switching model of similarity-assisted RNA recombination. In summary, PRRSV readily undergoes nonhomologous RNA recombination to generate heteroclite subgenomic RNAs. 

## INTRODUCTION

Porcine reproductive and respiratory syndrome virus (PRRSV) is a major infectious threat to the swine industry. The disease first appeared approximately 1 decade ago in both the United States (Collins *et al.,* 1992; Keffaber, 1989) and Europe (Wensvoort *et al.,* 1991) but is now endemic worldwide, despite serious efforts at control. PRRSV is classified as one of four members of the newly established family *Arteriviridae* (Meulenberg *et al.,* 1993b; Nelsen *et al.,* 1999), which also includes lactate-dehydrogenase elevating virus (LDV), equine arteritis virus, and simian hemorrhagic fever virus (Plagemann and Moennig, 1992). Along with *Coronaviridae* and *Toroviridae, Arteriviridae* belong to the order *Nidovirales* (Cavanagh *et al.,* 1990). While the complete genomes of many arteriviruses are known (Allende *et al.,* 1999; Godeny *et al.,* 1990; Meulenberg *et al.,* 1993b; Nelsen *et al.,* 1999; Palmer *et al.,* 1995; van Dinten *et al.,* 1997), much remains to be elucidated concerning viral interactions with the macrophage host. One step toward understanding these interactions is to identify all viral transcripts and proteins produced during natural infection.

All members of the order *Nidovirales* are single-stranded positive-sense RNA viruses that produce a nested set of subgenomic RNAs in the infected cell. PRRSV contains a genome of approximately 15 kb in length and has evolved separately in the United States (prototype strain VR-2332; Murtaugh *et al.,* 1995; Nelsen *et al.,* 1999) and Europe (prototype strain Lelystad; Meulenberg *et al.,* 1993b), such that two very distinct genetic types have emerged (Murtaugh *et al.,* 1995; Nelsen *et al.,* 1999). However, these two distinct types retain similar genomic organization (Conzelmann *et al.,* 1993; Meng *et al.,* 1994; Meulenberg *et al.,* 1993b; Murtaugh *et al.,* 1995; Nelsen *et al.,* 1999). The PRRSV genome encodes a large viral replicase (open reading frames (ORF) 1a and 1b) which is expressed from the genomic RNA and several major nested, 3′ coterminal subgenomic mRNAs (sg mRNAs). All of the sg mRNAs, except the smallest, are polycistronic. The major sg mRNAs encode, from largest to smallest, four glycoproteins (GP2–GP5; ORFs 2–5, respectively), an unglycosylated membrane protein (M; ORF 6), and a nucleocapsid protein (N; ORF 7) (Conzelmann *et al.,* 1993; Meng *et al.,* 1994; Meulenberg *et al.,* 1993b; Murtaugh *et al.,* 1995; Nelsen *et al.,* 1999). Minor sg mRNA transcripts are also observed (Meng *et al.,* 1996; Nelsen *et al.,* 1999), and the virus also contains several ORFs for which no protein product has been identified. Each sg mRNA is formed by an unclear mechanism of discontinuous transcription, but appears to involve sense and antisense base pairing of transcription-regulating sequences (van Marle *et al.,* 1999). All strain-

[1] To whom correspondence and reprint requests should be addressed. Fax: (612) 625-5203. E-mail: kay@lenti.med.umn.edu.

0042-6822/00 $35.00

specific viral RNAs possess identical 5′ and 3′ regions with small ORFs for which no concrete function has been determined (Allende *et al.,* 1999; Meulenberg *et al.,* 1993a; Nelsen *et al.,* 1999).

All Nidoviruses undergo RNA genome recombination. Such recombination can be classified as homologous or nonhomologous, based on the nature of the RNAs involved and the degree of homology in the crossover region (Lai, 1992, 1996; Nagy and Simon, 1997). The vast majority probably arise by a "polymerase copy-choice" or "template switching" mechanism, as originally proposed by Huang (Huang, 1977). Homologous recombination involves two similar or closely related RNAs with high homology and the crossovers occur at perfectly matched sites so that resultant recombinant RNAs retain the exact sequence and structural organization of parental RNA molecules. Homologous recombination is believed to be one of the major mechanisms used by the positive-stranded RNA viruses to maintain genetic stability, rescue genomes of nonviable progeny RNA, and generate sequence variants to evade immunogenic pressure (Nagy and Simon, 1997). Nonhomologous recombination occurs between two different sites of the same or different RNAs without apparent homology at the crossover site so that the resultant recombinant virus contains insertions or deletions. The most commonly observed incidence of nonhomologous recombination is the production of defective interfering (DI) RNAs during high-multiplicity viral infection. By definition, DI RNAs are those mutants that usually contain multiple internal deletions but retain the *cis*-acting elements essential for replication, such as regions of the polymerase, the nucleocapsid gene, and the viral packaging signal. DI RNAs are, therefore, an important tool to help define the *cis*-acting signals that regulate the viral life cycle.

Coronaviruses undergo high-frequency RNA recombination (Jia *et al.,* 1995; Keck *et al.,* 1988; Lai *et al.,* 1985; Masters *et al.,* 1994; Wang *et al.,* 1993; reviewed in Lai, 1996) and produce DI RNAs. Naturally occurring DI RNAs, ranging from 2.2 to 28 kb in length, have been identified for four coronaviruses, mouse hepatitis virus (MHV) (Makino *et al.,* 1985, 1988; van der Most *et al.,* 1991), infectious bronchitis virus (IBV) (Penzes *et al.,* 1994), bovine coronavirus (BCV) (Chang *et al.,* 1994), and transmissible gastroenteritis virus (TGEV) (Mendez *et al.,* 1996), and have been instrumental in determining regulatory *cis*-acting sequences for coronavirus replication and transcription. All described coronaviral DI RNAs identified were selected after repeated high-multiplicity passage and were found to contain mostly multiple discontinuous genomic regions, but to have retained similar viral 5′ and 3′ ends (Chang *et al.,* 1994; Makino *et al.,* 1985, 1988; Mendez *et al.,* 1996; Penzes *et al.,* 1994; van der Most *et al.,* 1991).

Recently, arteriviruses PRRSV (Yuan *et al.,* 1999) and LDV (Li *et al.,* 1999) were also shown to undergo homologous recombination, but the appearance of DI RNAs was not reported. Since the production of defective interfering viral particles is a well-recognized consequence of passaging virus at high multiplicity of infection (m.o.i.), we hypothesized that PRRSV might also undergo nonhomologous RNA recombination to generate DI RNAs that would be enriched during high m.o.i. infection. Potential PRRSV DI RNAs, like coronaviral DI RNAs, would retain the 5′ and 3′ regions with variable internal deletions. We found nine abundant "DI-like" subgenomic RNAs in cells and purified virions following high m.o.i. infections of MA-104 cells. However, the subgenomic RNAs were not characteristic DI RNAs. They were present under conditions of low m.o.i. infection and present both in virus isolated directly from the field and in plaque-purified virus. In addition, none of the subgenomic RNAs contained the ORF 1b sequence encoding the polymerase and helicase. The subgenomic RNAs were further distinguished from standard nidovirus DI RNAs since the joining of 5′ and 3′ ends occurred at sites of nucleotide sequence identity (Brian and Spaan, 1997; van Marle *et al.,* 1999). Therefore, these subgenomic RNAs are not typical with respect to other nidovirus DI RNAs and require discrete regions of nucleotide identity to effect nonhomologous recombination. We propose the term "heteroclite RNA" (meaning "deviating from common forms or rules") to refer to these novel PRRSV RNA species.

## RESULTS

### Sequential passage of PRRSV

Titration of virus from serial passage at both low (0.001) and high m.o.i. (2.5) exhibited similar patterns of viral RNA replication. The degree of titer fluctuation (5- to 10-fold for low m.o.i., 5- to 15-fold for high m.o.i.) was comparable to that observed in other *Nidoviridae* species where DI RNAs have been detected (data not shown; Makino *et al.,* 1984; Snijder *et al.,* 1991). However, the kinetics of cytopathogenicity were accelerated during high m.o.i. passages such that cytopathic effect appeared approximately 1 day earlier than CPE of low m.o.i. infections, and high-multiplicity passage often resulted in higher progeny titers. This suggested that defective RNAs, if present at high m.o.i. passage and absent at low m.o.i. passage, did not negatively influence viral growth kinetics or decrease virus yield.

### Northern blot analysis of PRRSV-infected total cellular RNA

To obtain evidence that defective RNAs were generated during serial passage at high m.o.i., total cellular RNA from MA-104 cells infected with sequential high (2.5) m.o.i. passages of VR-2332, plaque-purified virus, or mock-infected control cells were electrophoresed in trip-

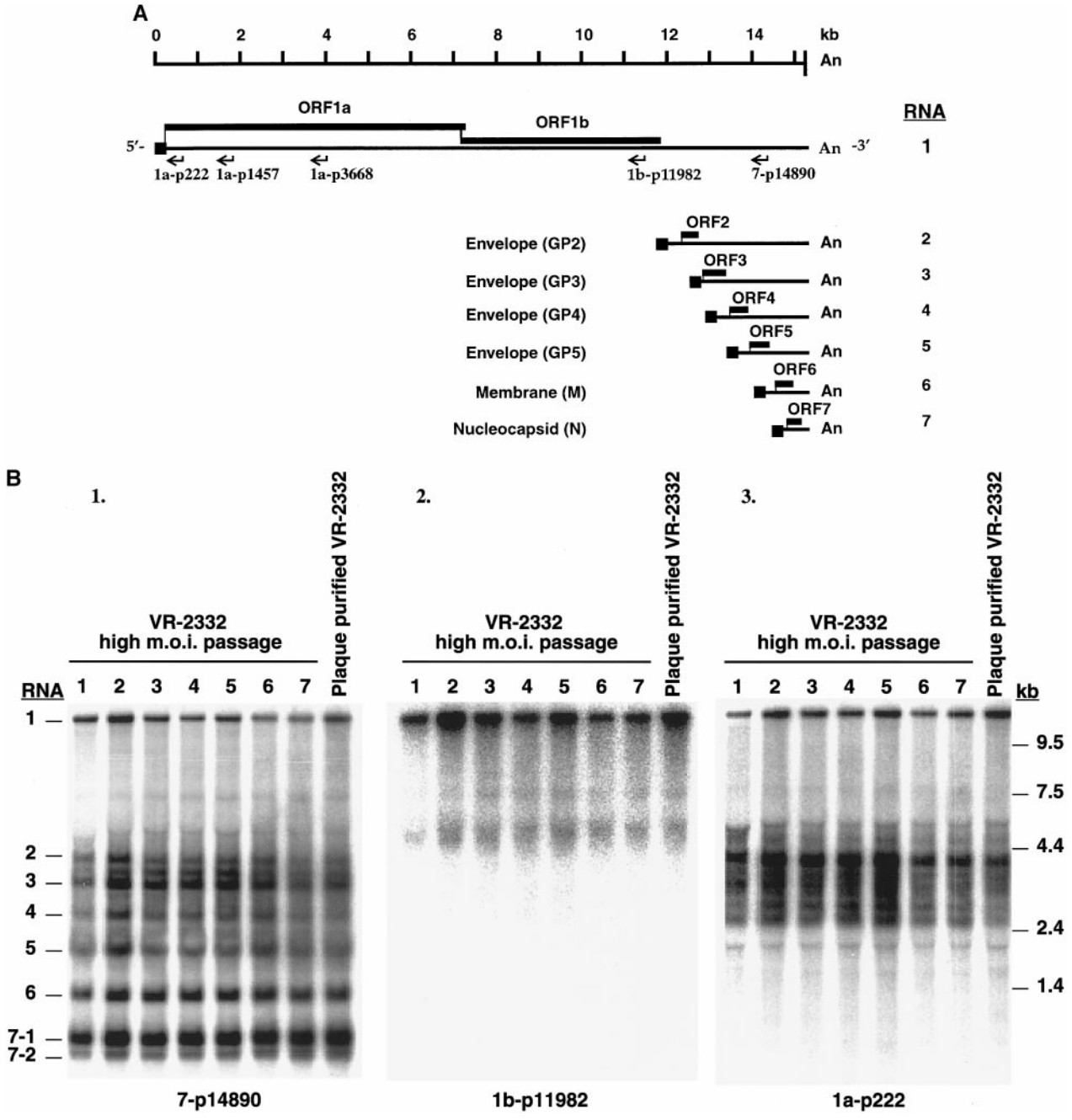


FIG. 1. A. Schematic of the arteriviral transcription strategy showing the placement of VR-2332 ORF-1-specific and ORF-7-specific probes synthesized and used for Northern blot analysis. B. MA-104 cell total RNA after infection by PRRSV strain VR-2332 passages 1–7 (lanes 1–7) or by plaque-purified virus (lane 8) was isolated, electrophoresed in triplicate, and blotted as described. Probes were prepared for detection of RNA species containing the ORF 7 sequence (1, 7-p148901), ORF 1b sequence (2, 1b-p11982), or ORF 1a sequence (3, 1a-p222).

licate, blotted onto nylon membranes, and analyzed for the presence of VR-2332-specific sequences. Synthetic oligonucleotide probes that were complementary to different genomic regions of VR-2332 RNA were prepared and radiolabeled as described (Table 1, Fig. 1A). A probe specific for the ORF 7 sequence (7-p14890) detected numerous extra subgenomic RNA species in addition to the viral genomic RNA and subgenomic mRNAs 2-7 (Fig. 1B1). When identical lanes were probed for a sequence in ORF1b (1b-p11982) only genomic RNA was readily detected, but fewer abundant large RNA species were also observed (Fig. 1B2). The third set of lanes, probed with a radiolabeled oligonucleotide complementary to the 5′ end of ORF 1a (1a-p222), unexpectedly revealed at least nine abundant subgenomic length RNA species (Fig. 1B3).

In order to demonstrate that the ORF 1a-specific subgenomic RNA bands were only propagated under con-

ditions of high m.o.i. passage, RNA from MA-104 cells infected by plaque-purified VR-2332 was also analyzed. Surprisingly, the plaque-purified virus produced very similar RNA species to those seen in high m.o.i. viral passage (Fig. 1B, lane 8). Mock-infected MA-104 cells did not contain analogous RNA bands (data not shown). To control for ORF 1 probe specificity, the ORF 1a and ORF 1b probes were tested for hybridization to *in vitro* transcribed subgenomic ORF 2 RNA. No cross-reactivity was observed (data not shown). The results demonstrated that these ORF-1a-containing subgenomic-length RNAs, most often termed defective RNAs, were generated by a single round of cultured cell infection by three times plaque-purified VR-2332, as well as by serial high-multiplicity VR-2332 passages. Despite extensive investigation, culture conditions were not identified in which these RNA species were eliminated, thus indicating that production of the atypical subgenomic RNAs was an inherent aspect of PRRSV replication or transcription or both.

### Atypical RNA species are produced by other cell-adapted PRRSV strains

To gain additional evidence that the development of these RNAs was not dependent on multiplicities of infection or passage number, we electrophoresed and blotted intracellular RNAs from MA-104 cells infected with VR-2332 at different multiplicities of infection or at different passages, or cells infected with two cell-adapted attenuated virus strains (RespPRRS and Prime-Pac PRRS). Using the same radiolabeled oligomer complementary to ORF 1a (1a-p222), abundant subgenomic-length RNAs were detected under all conditions (Fig. 2). VR-2332 infection produced the same pattern of RNA bands in these cells, whether passaged once at high multiplicity (2.5 m.o.i.; lane 1), 19 times at high (lane 2) or low (0.001 m.o.i.; lane 3) multiplicity, or once at low multiplicity with plaque-purified virus (lane 4). We identified the nine most distinct VR-2332 atypical species detected (I-1 to I-9). Twelfth-passage RespPRRS (lane 5) and 14-passage Prime Pac PRRS (lane 6) vaccine strains also generated similar RNAs, although the ORF-1a-specific subgenomic RNA pattern produced in Prime Pac PRRS-infected cells differed with the RNA pattern generated by infection of VR-2332 and its derivative RespPRRS. No RNA bands were observed when uninfected cells were similarly analyzed (lane 7). These results suggested that the production of subgenomic-length ORF-1a-specific RNAs may be a general property of PRRSV infection in culture on MA-104 cells.

### Atypical subgenomic-length RNAs are also produced in porcine macrophages, the natural host cell

To assess whether the ability of PRRSV-infected cells to produce these unusual RNA species was limited to *in vitro* growth, we electrophoresed RNA from freshly isolated porcine lung macrophages that remained uninfected or had been infected with a variety of PRRSV field isolates that had never been propagated in cultured cells. When hybridized to probe 1a-p222, subgenomic-length RNA bands were detected for field isolates 99-88766, 99-13084, and 96-26663 (a neurovirulent isolate; Rossow *et al.,* 1999) that comigrated with RNA species produced by VR-2332-infected MA-104 cells (Fig. 3). The data suggest that such RNA bands may be present and formed by the same mechanism during natural PRRSV infection.

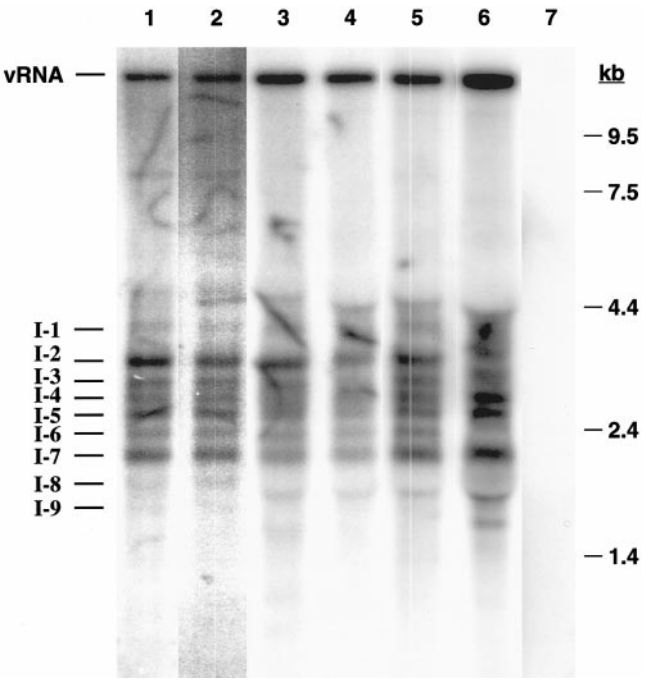


FIG. 2. PRRSV infection of MA-104 cells at different passage numbers reveals novel RNA species. Total RNA was isolated, electrophoresed, and blotted and then probed with radiolabeled oligomer 1a-p222. Nine new prominent subgenomic RNAs were detected in MA-104 cells infected with plaque-purified VR-2332 (0.001 m.o.i.; lane 1), p1 at 2.5 m.o.i. (lane 2), VR-2332 p19 at 2.5 m.o.i. (lane 3), VR-2332 p19 at 0.001 m.o.i. (lane 4), RespPRRS vaccine strain p12 (0.001 m.o.i.; lane 5). A different pattern of subgenomic RNAs were also detected in Prime-Pac PRRS vaccine strain p12 (0.001 m.o.i.; lane 6). Total RNA from mock-infected MA-104 cells was used as a control (lane 7).

### Atypical subgenomic-length RNA species contain internal deletions but retain 5′ leader, 3′ UTRs, and ORF 7 regions

To assess the primary structure of these intracellular RNA species, we synthesized a series of oligonucleotide probes complementary to each coding region of the full-length genome of PRRSV (Table 1) and conducted Northern blot analysis of total cellular RNA infected by strain VR-2332 for 21 passages at high (2.5) m.o.i. (Fig. 4). In an effort to clarify the results of Fig. 4, we digitally adjusted the level of hybridization intensities to equalize

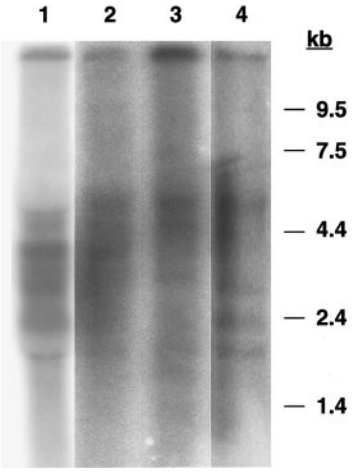


FIG. 3. PRRSV infection of porcine alveolar macrophages reveals that atypical subgenomic RNA bands are present in host cells. Total RNA was isolated from cells, electrophoresed, blotted, and probed with radiolabeled oligomer 1a-p222. PRRSV p19-infected MA-104 cell RNA (2.5 m.o.i.; lane 1) or RNA from porcine alveolar macrophages that was infected with PRRSV original VR-2332 field isolate passaged in macrophages three times (lane 2), neurovirulent field isolate UM96-26663 (lane 3), and field isolate UM-13284 (lane 4).

the full-length viral RNA message detected in each lane. No hybridization bands disappeared in this process. All RNA species, including subgenomic mRNA 2-7 and the newly identified RNA species, contained sequences within the PRRSV leader, ORF 7 region, and 3′ untranslated region (Fig. 4; lanes 1, 11, and 12, respectively). Again, the atypical subgenomic RNAs were detected by 1a-p222 (nt 222–261), indicating that they contained the PRRSV genomic sequence from the 5′ end of ORF 1a, which is absent in subgenomic mRNAs 2–7 (Fig. 4, lane 2). The most abundantly detected intracellular RNA bands were designated I-2, I-5, and I-7 (I = intracellular; approximately 3.8, 2.4, and 1.9 kb, respectively). However, the downstream ORF 1a sequence at nucleotides 1457–1494 (probe 1a-1457) was not detected in some of the smaller atypical subgenomic RNA bands such as I-7 (Fig. 4, lane 3). Furthermore, the VR-2332 sequence at nucleotides 3668–3707 and 11982–12003 was not identified in the majority of the atypical subgenomic RNA species (Fig. 4, lanes 4 and 5). These results suggested that the 5′ boundaries of atypical RNA species were within the 5′-end of ORF 1a. Similarly, the data obtained using probes complementary to ORF 2–7 indicated that the majority of these RNAs did not contain sequences within ORF 2, 3, or 4 and therefore appeared to only harbor sequences downstream of ORF 4. The Northern blot data further confirmed that the atypical RNA species contained large internal deletions. The data corresponding to atypical subgenomic RNA species I-2, I-5, and I-7 are summarized in graphic form at the bottom of Fig. 4. Size estimates of the hybridizing bands, combined with the known locations of the oligonucleotide probes, indicated that the atypical subgenomic RNAs detected in the infected cell were composed exclusively of 5′ and 3′ genomic sequences. However, the possibility existed that small discontinuous regions of internal genomic sequence existed in the undetermined bases.

## PRRSV atypical subgenomic RNAs are packaged into virions

Nested PCR was conducted to assess whether intracellular atypical RNAs were packaged into virions. First-round PCR was performed using a leader primer (658p5) and Qi (Table 1) on cDNA prepared from intracellular PRRSV RNA or RNA harvested from extracellular virus that was purified by sucrose cushion centrifugation. First-round products were amplified by a second round of PCR using the primer pair, 5′382 (ORF 1a specific, VR-2332 nt 382–402) and p75 (ORF 7 specific, nt 15139–15158). Both intracellular and extracellular RNA templates yielded several DNA products (Fig. 5), whereas uninfected cell RNA did not yield any product (data not shown). The pattern and sizes of the PRRSV-infected intracellular RNA products (Fig. 5, lane 1) were consistent with the ORF-1a-specific atypical RNA bands detected in Northern blot analysis (Figs. 2 and 4), including a band (I2-7, 1.9 kb) similar in size to the I-7 band (Figs. 2 and 4). Furthermore, the RNA harvested from purified virions produced comparably sized products (Fig. 5, lane 2). These products were designated S-1 through S-7 (S = supernatant). Increasing the time of ultraviolet light exposure of lane 2 revealed two additional RT-PCR bands, S-8 and S-9. We previously showed that PRRSV intravirion RNA is protected from RNase degradation while extravirion RNA is not (Yuan *et al.,* 1999). However, to solidify the finding that these atypical subgenomic RNAs were packaged, infected cell medium supernatant was incubated with and without the addition of RNAseA (140 ng/$\mu$l) for 1 h at 37°C prior to viral RNA isolation and RT-PCR. Identical results were obtained regardless of the presence of RNAse A. This result was due to the protection of atypical subgenomic RNA within virions, since purified RNA added to the culture medium in the presence of RNAse A was completely degraded (data not shown). RT-PCR analysis of a second PRRSV strain, PrimePac PRRS, revealed an equivalent pattern of subgenomic RNA bands in virus purified from the medium of infected cells (data not shown). Therefore, the results indicated that atypical PRRSV RNA species were packaged into virions.

## Nucleotide sequence of atypical subgenomic RNA species

Individual atypical RNA species were PCR amplified, cloned, and sequenced to obtain the primary structure of the novel RNAs. DNA bands I2-7, S-2, and S-7 through S-9 (Fig. 5) were gel-purified and cloned into bacteria.

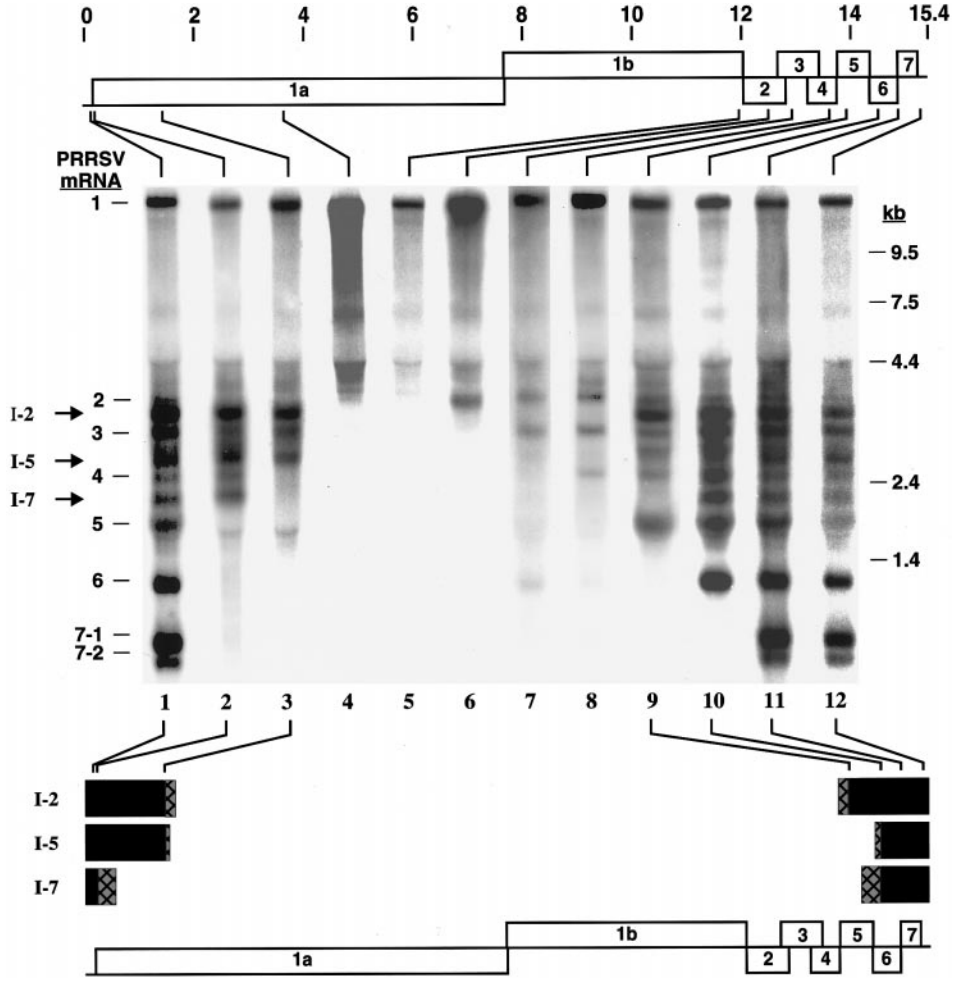


FIG. 4. Northern blot hybridization results suggest that atypical RNAs contain one large internal deletion. Total cellular RNA was isolated from MA-104 cells infected with VR-2332 p19 at high m.o.i., electrophoresed in 12 separate lanes, and transferred to a nylon membrane. Radiolabeled region-specific probes for the 5′-leader sequence (Leader-p150, lane 1); ORF 1a nucleotides 222–261 (1a-p222, lane 2), 1457–1494 (1a-p1457, lane 3), and 3668–3707 (1a-p3668, lane 4); ORF 1b (1b-p11982, lane 5); ORF 2 (2-p12516, lane 6); ORF 3 (3-p12949, lane 7); ORF 4 (4-p13636, lane 8); ORF 5 (5-p13942, lane 9); ORF 6 (6-p14525, lane 10); ORF 7 (7-p14890, lane 11); and the 3′ untranslated region (lane 12). Bars at the top represent the placement of a specific probe on the genome and its corresponding lane, and those at the bottom represent probe-positive regions for specific atypical RNAs (I-2, I-5, I-7) and the deduced primary structures of those RNAs. Solid bars signify regions positive by hybridization and cross-hatched bars signify the probable sequence needed to code for the correct nucleotide length.

Nucleotide sequencing of the resultant plasmids was completed to examine the entire PRRSV insert. The lengths of I2-7, S-2, and S-7 through S-9 from sequence analysis correlated accurately to the sizes predicted from Northern blot (I-7) and RT-PCR analyses (I2-7, S-5, and S-7 through S-9). In all cases, the determined sequences revealed that the atypical subgenomic RNAs were composed of only two genomic regions of PRRSV, reflecting the junction of 5′-ORF 1a nucleotides with downstream sequences in the 3′-end of the genome. The junction site was distinct in most cases and existed at sites of short (3–7 nucleotides) sequence identity between the specific 5′ and 3′ PRRSV genomic regions (Fig. 6A). Heterogeneity was observed in the junction site location and sequence in subgenomic RNAs cloned from the same size class, as demonstrated in sequence analysis of two subgenomic-length virion RNA gel bands (S-7a and S-7b, S-9a and S-9b) (Fig. 6A). In addition, we found an intracellular atypical RNA species (I2-7) which was identical in sequence to a virion-derived atypical RNA (S-7b), consistent with the packaging of intracellular atypical subgenomic RNA. It appears that the RT-PCR bands may represent a mixture of similarly sized RNAs and that the sequences joining the 5′ and 3′ ends are variable and different than the consensus VR-2332 transcriptional leader–body junction sequence UUAACC.

All atypical RNA molecules examined were joined within the ORF 1a coding sequence and possessed all known regions required for translation. The first reading frame of each of the subgenomic RNA transcripts coded for a putative protein containing truncated ORF 1 protein fused with downstream amino acids located in alterna-

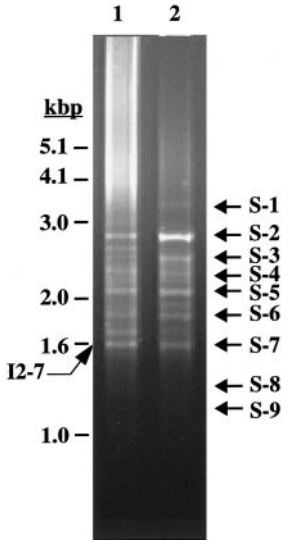


FIG. 5. VR-2332 p19-infected MA-104 cell total RNA (lane 1) or RNA from virus isolated from the supernatant (lane 2) produced similar RT-PCR products. S-8 and S-9 were visible only on prolonged exposure of the gel. DNA bands I2-7, S-2, and S-7 through S-9 were purified and sequenced.

tive reading frames or fused in-frame to ORF 6 amino acids (Fig. 6B). We noted that one or both papain-like cysteine protease cleavage sites were present in five of the predicted polypeptides (den Boon *et al.,* 1995; Nelsen *et al.,* 1999).

## DISCUSSION

Most defective RNAs interfere with the replication of their parental viruses, which results in fluctuation of the virus titers among serial passages at high m.o.i. infection. The defective RNAs of coronaviruses and toroviruses, such as MHV (Makino *et al.,* 1984, 1988) and Berne virus (Snijder *et al.,* 1991), showed some (approximately 10-fold) or no (IBV; Penzes *et al.,* 1994) ability to interfere with viral replication at high m.o.i. Defective interfering RNAs of the coronavirus, TGEV (Mendez *et al.,* 1996), also display interference with helper genomic and subgenomic RNA synthesis, suggesting that viral replication is also affected. Finally, in BCV (Chang *et al.,* 1994), a defective RNA species was present in the stock strain derived from three times plaque-purified virus, but no viral replication information was reported. Thus, it is difficult to define unifying qualities of the coronaviral defective interfering RNAs studied to date (Brian and Spaan, 1997).

We identified several novel PRRSV subgenomic RNAs that were constitutively present during serial passage at high and low multiplicities of infection in MA-104 cells and were demonstrated in several PRRSV field strains that had not been cell cultured. These atypical transcript species are distinct from "defective interfering RNAs" in that plaque purification did not clear these RNAs from viral stocks, interference specific to repeated high-multiplicity passage was not observed, and the subgenomic RNAs were present in virus isolated directly from the field. In contrast to the majority of coronavirus-defective RNAs that inhibit the transcription of all (Mendez *et al.,* 1996) or all but ORF 7 mRNA (Makino *et al.,* 1990), PRRSV atypical subgenomic RNAs coexist with apparently normal levels of genomic RNA and major subgenomic mRNAs. This suggests that the modest fluctuations seen in PRRSV growth on MA-104 cells were probably not due to specific inhibition of major subgenomic mRNA synthesis by PRRSV atypical subgenomic RNAs. Last, each of the sequenced atypical subgenomic RNAs was found to contain only a contiguous sequence from the 5′ and 3′ ends of the viral genome, with a single large internal deletion. This feature also describes the major subgenomic mRNAs of PRRSV (sg mRNA2–7). However, the RNAs described here have an additional 5′ ORF 1a sequence and appear to result from single recombination events at heterogeneous sites, rather than single recombination events at a predicted consensus sequence (UUAACC). Defective RNA species of this type have been described for two other Nidoviruses, yet those particular RNA species either resulted from high-multiplicity passage and were related to passage number (Berne virus; Snijder *et al.,* 1991) or were a transient observation in persistently infected cells (BCV; Hofmann *et al.,* 1990). We propose that the PRRSV atypical RNA species described in this report be termed heteroclite (meaning "deviating from common forms or rules") subgenomic mRNAs because they result from single RNA recombination events similar to the proposed formation of the major subgenomic mRNAs, do not contain regions of ORF 1b shown to be critical in the formation of most coronaviral defective RNAs, seem to be constitutively present in infected cells, and are formed by a process with features of both homologous and nonhomologous recombination. The PRRSV polymerase may be more adept in switching templates than the typical coronavirus polymerase, so that instead of occasional defective coronavirus RNAs arising from high-multiplicity passage, we see continual propagation of heteroclite subgenomic RNAs under low- as well as high-multiplicity passage. These subgenomic RNAs could thus have become part of the natural PRRSV infection.

The biological function of the PRRSV heteroclite subgenomic mRNAs is unknown, but they may be an important factor contributing to the relative virulence and/or persistence of specific strains of virus, play a role in viral replication, or be a unnecessary product of RNA replication in host cells due to an errant polymerase. For strain VR-2332, each of these RNA species is heterogeneous in size and sequence and codes for different protein products. The atypical RNAs may be present to increase the amount of the 5′-end ORF 1a proteins, whose function is unknown, delineated by the papain-like cysteine pro-

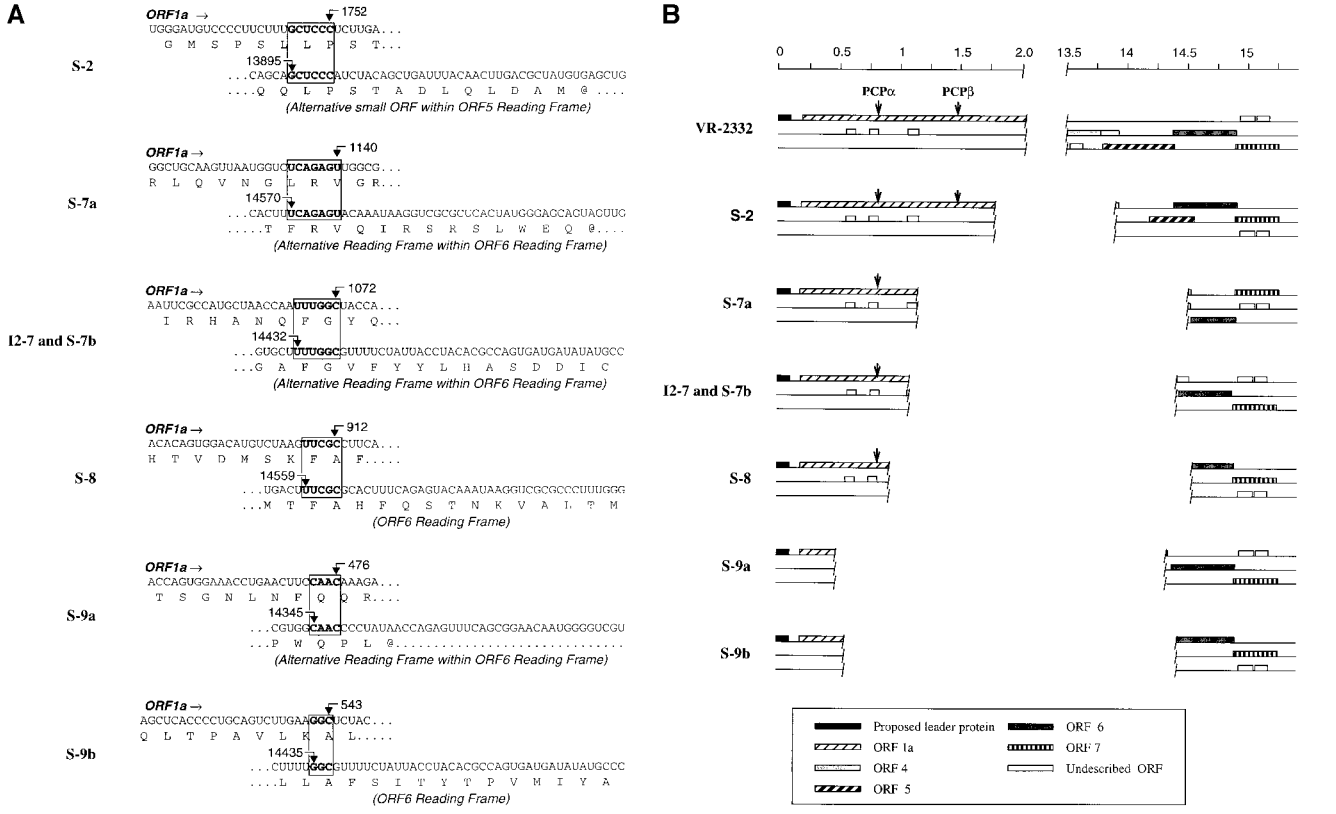


FIG. 6. A. Sequence analysis reveals that atypical subgenomic mRNAs have one large internal deletion and are joined at aberrant 5′–3′ junction sites that consist of heterogeneous nucleotides. Purified DNA bands were cloned into bacteria and one or two clones were selected and sequenced. The figure represents the sequences of the crossover regions (boxed) for six clones (S-2, S-7a and -b, I2-7, S-8, S-9a and -b; S = supernatant, I = intracellular) and the predicted polyproteins with corresponding base numbers displayed above the sequence. The presumed fusion polypeptide product is identified in parentheses below each sequence. B. Translation of the sequenced heteroclite RNAs in all three frames suggest that additional 5′ papain-like protease (PCP$\alpha$ and PCP$\beta$) cleavage products and/or fusion proteins may be produced in the infected cell.

tease cleavage sites. These novel RNAs may also express minor levels of a PRRSV fusion protein. However, if the ribosome, when translating viral transcripts, were to occasionally read through to the two remaining reading frames or to translate downstream ORFs, additional proteins may be expressed (Fig. 6B, open boxes). The ability of arteriviruses to undergo ribosomal frameshifting during translation has been shown previously (den Boon *et al.,* 1991; Snijder *et al.,* 1999). The two vaccine strains contain a similar profile of heteroclite RNAs, but the particular vaccine heteroclite subgenomic RNAs have not been studied in detail in order to link them to attenuation. Additional analysis of comparably sized RT-PCR products of different strains may help define a functional role.

We demonstrated that these heteroclite RNAs were protected from RNAse A degradation in the infected cell supernatant, providing strong evidence that these RNA species are packaged into virus-like particles. Because these heteroclite subgenomic RNAs are packaged, they may be used in encapsidation studies to define *cis*-acting signals for replication and packaging. The heteroclite subgenomic RNAs were detected in sucrose-gradient-purified virions, but were also detected in other portions of the gradient and will need to be further examined (data not shown). However, as all of the atypical subgenomic RNAs appeared to contain an intact 5′-end of the PRRSV genome and the major subgenomic mRNAs (mRNAs2–7) are not packaged, we suggest that the viral RNA encapsidation signal most likely resides in the 5′-end of ORF 1a, between nucleotides 190 and 476, as S-9a was the shortest atypical RNA isolated from packaged virus. An alternative explanation is that efficient viral packaging may consist of several factors and that the sequence at the 5′-end of ORF 1a may interact with a specific packaging signal located further downstream. The packaging signals for MHV JHM strain (Makino *et al.,* 1985, 1990), MHV A-59 strain (van der Most *et al.,* 1991), and BCV (Cologna and Hogue, 2000) were identified in specific regions of ORF 1b.

We have also studied the aberrant 5′–3′ junction sites present in PRRSV atypical subgenomic RNAs. It is interesting that the sequences mediating the junction site do not display any similarity to the traditional leader–body junction used by this virus, UUAACC. Instead, they display heterogeneity in size and sequence and no obvious

base-pairing immediately outside of the region of identity. The 5′ and 3′ end joining involves direct base-pairing between sense and antisense viral strands, but secondary structures also appear to play a substantial role in defining the site of sense–antisense interaction (Brian and Spaan, 1997; van Marle *et al.,* 1999). We have generated RNA folding patterns for the regions surrounding the atypical subgenomic RNA junction sites and find that these junction sites, as well as the major leader–body junction sites for ORFs 2–7 mRNAs, often occur at unpaired nucleotides within hairpins of predicted stability and believe that "kissing loops" (Chang and Tinoco, 1994) may play a role in forming 5′–3′ junctions. Our results support a model in which PRRSV RNA secondary structures play a most critical role in this interaction, as the arteriviral RNA polymerase seems to be able to jump to regions of minimal sequence similarity (as few as three nucleotides). Other viral or host proteins also may play a fundamental role in accurately directing this RNA-directed RNA polymerase to the correct site for subgenomic mRNA formation. However, the polymerase may occasionally subvert the prevalent method of junction site formation and make an incorrect leap. This may explain the formation of defective interfering RNAs in other nidoviruses.

## MATERIALS AND METHODS

### Viruses and cells

PRRSV strains VR-2332 (cloned virulent field strain), RespPRRS (Boehringer Ingelheim Animal Health, St. Joseph, MO) vaccine virus, and Prime Pac PRRS (Schering Plough Animal Health, Kenilworth, NJ) vaccine virus are cell-adapted viruses that were subjected to 7 or 71 passages on the MA-104 simian cell line or 94 passages on macrophages, respectively. The cells were maintained in EMEM medium containing 10% fetal bovine serum (FBS). For serial consecutive passaging, VR-2332 was used to infect MA-104 cells at low (0.001) and high m.o.i. (2.5) and incubated at 37°C, 5% $CO_2$, for 72 to 120 h postinfection (p.i.). For subsequent passages, 0.5 ml of diluted ($1 \times 10^{-3}$, low m.o.i) or undiluted (high m.o.i) supernatant was added to fresh monolayers of MA-104 cells (Penzes *et al.,* 1994). Titration of each passage supernatant revealed similar virus concentrations, regardless of the m.o.i. used. The infected cell supernatants were harvested when the cultures exhibited 80% cell cytopathic effect (CPE) and stored at −80°C. VR-2332 was also plaque purified by three rounds of plaque-to-plaque isolation. PRRSV field isolates were obtained from the University of Minnesota Veterinary Diagnostic Laboratory.

### Virus plaque assay and plaque purification

For virus titration, cell culture supernatants were diluted $10^3$–$10^6$ fold in EMEM without FBS. Diluted virus (50 μl) was added to duplicate wells of a 12-well-plate (Corning) which contained 90% confluent MA-104 cell monolayers, followed by room temperature (RT) incubation for 1 h with occasional redistribution of the inoculum. An equal mixture (1.5 ml) of 2 × EMEM medium and 2% SeaPlaque LE agarose (FMC), prewarmed at 56°C, was added to each well and then left at RT for 15 min to solidify the agarose overlay. The cells were then transferred for incubation at 37°C in 5% $CO_2$ for 96 h. To stain viral plaques, 100 μl of 3 mg/ml 3-[4,5-dimethylthiazol-2-yl]-2,5-diphenyltetrazolium bromide (MTT, Sigma) was added to each well, and the plates were further incubated for 4 to 12 h. The results were recorded as the number of plaque forming units per milliliter of inoculum (PFU/ml). For VR-2332 plaque purification, a piece of agarose overlay plug on the top of a well-separated plaque was removed and resuspended into 200 μl of EMEM containing 2% FBS. Plaque purification was repeated twice more with $10^{-1}$ to $10^{-3}$ dilutions of suspension. To amplify the 3× plaque-purified viral stock, a $10^{-3}$ diluted suspension was used to infect $2 \times 10^7$ MA-104 cells. The cell supernatant was harvested 3 days later, aliquoted, and stored at −80°C.

### Intracellular RNA purification

At 36 h p.i., total cellular RNAs from $2 \times 10^7$ MA-104 cells, mock infected or infected with PRRSV at low or high m.o.i., were isolated using a RNAeasy Midi kit (QIAgen Inc.). Briefly, the cell monolayer was washed with phosphate-buffered saline and harvested using a rubber policeman. The harvested cells were lysed in supplied buffer (RLN) and homogenized by passage through a 20-gauge needle 20 times. The lysates were loaded onto a spin column and subjected to two rounds of washing with buffer (RW1). Elution buffer or DEPC-treated $H_2O$ (60 to 100 μl) was used to elute the purified RNAs.

### Purification of viruses and viral RNAs

For large-scale preparation of viruses, $1.2 \times 10^8$ MA-104 cells were infected as described above. The infected cell supernatants were harvested at 96 h p.i., when 80% CPE was observed. Cellular debris was pelleted by centrifugation at 15,000 rpm in a Beckman JA20 rotor for 20 min and the supernatants were then loaded onto a 0.5 M sucrose/10 mM Tris (pH 7.5)/10 mM NaCl/1 mM ethylenediaminetetraacetic acid cushion in a Beckman SW 27 tube and centrifuged at 24,000 rpm for 16 h in a Beckman L8-60M ultracentrifuge to pellet virions. The pellet was resuspended in 1 to 2 ml of 0.1 M LiCl/5 mM EDTA/1% sodium dodecyl sulfate (SDS) and viral RNA was purified as described (Nelsen *et al.,* 1999) and stored at −80°C. Purification of intravirion RNA free from extraneous RNA contamination was accomplished by treatment with RNAse A (140 ng/μl, 1 h at 37°C) prior to RNA extraction (QIAamp viral RNA purification kit, QIAgen Inc.).

TABLE 1

Oligonucleotides Used in Northern Blot Hybridization and RT-PCR Studies

| Name | Sequence | VR-2332 nucleotide |
|---|---|---|
| Leader-p21 | 5′-TCTATGCCTTGGCATTTGTATTG | 21–43 |
| Leader-p150 | 5′-GTTAAAGGGGTGGAGAGACCGTAAAGCAGTGCAACTCCGG | 150–190 |
| 1a-p222 | 5′-TAGACTTGGCCCTCCGCCATAAACACCCTGGCATTGGGGG | 222–261 |
| 5′-382 | 5′-ATTCCCCACTGTTGAGTGCTC | 382–402 |
| 5′-804 | 5′-GCGGGGATGAAGTGAA | 804–819 |
| 1a-p1457 | 5′-CCTTCGGCAGGCGGGGAGTAGTGTTTGAGGTGCTCAGC | 1457–1494 |
| 1a-p3668 | 5′-GGTCGTTGACAAGTTGGTCATCTACCGGTTTATCCTCGGA | 3668–3707 |
| 1b-p11982 | 5′-GTGGCAGTGGCCTTATAAATTTTCCCTTCC | 11982–12003 |
| 2-p12516 | 5′-TATTTACAGGTCTCGGCTTCAATGGCGGCTAGATGCTGAA | 12516–12555 |
| 3-p12949 | 5′-GGCCAGGCGGTATCATAAACCCTAGCTCGTCATGATCGTC | 12949–12961 |
| 4-p13636 | 5′-GAGCGTTGGGTAAACTCCTTGACATGTTGGACGTAGCTGG | 13636–13675 |
| 5-p13942 | 5′-CCACTGCCCAATCAAATTTGTTAGCTAGCCAATCTGTGCC | 13942–13981 |
| 6-p14525 | 5′-CGCGAAAGTCATGTACCCGAAGGTGAAAGCACAATTCAGG | 14525–14564 |
| 7-p14890 | 5′-CCTTCTTTCTCTTCTGCTGCTTGCCGTTGTTATTTGGCAT | 14890–14929 |
| p75 | 5′-GTGCAAGTCCCAGCGCCTTG | 15142–15161 |
| 3′UTR-p15299 | 5′-GCACAATGTCAATCAGTGCCATTCACCACACATTCTTCC | 15299–15337 |
| Qt | 5′-CCAGTGAGCAGAGTGACGAGGACTCGAGCTCAAGC(T)17 | — |
| Qo | 5′-CCAGTGAGCAGAGTGACG | — |
| Qi | 5′-GAGGACTCGAGCTCAAGC | — |

## Northern blotting analysis

RNA samples (10 $\mu$g) were denatured in 10 mM sodium phosphate buffer (pH 7.0), 50% dimethyl sulfoxide, and 0.9 M deionized glyoxal followed by incubation at 50°C for 1 h. The denatured samples were electrophoresed for 3–4 h through a 1% agarose gel in recirculating 10 mM sodium phosphate buffer (pH 7.0). The separated RNAs were transferred by capillary action onto a nylon membrane (MSI) as described previously (Nelsen *et al.,* 1999). Oligonucleotide probes complementary to individual genomic regions of PRRSV RNA (Table 1) were synthesized, 3′-end radiolabeled using terminal deoxynucleotide transferase (TdT, New England Biolabs) with [$\alpha^{32}$P]dATP (Amersham Life Sciences), and used for hybridization to the membrane-bound RNA in QuikHyb buffer (Stratagene) at 68°C. The membrane was washed three times in 0.9 M NaCl/0.09 M $Na_3$–citrate · $H_2O$/0.1% sodium dodecyl sulfate (SDS) at 68°C and then exposed to autoradiography film (NEN Life Science Products, Boston, MA) or a PhosphorImager screen (Molecular Dynamics).

## RT-PCR

Rapid amplification of cDNA ends (3′-RACE PCR) was performed on purified viral RNA templates or PRRSV-infected total cellular RNA with slight modification (Frohman, 1994). Qt primer (Table 1) was used to prime the RNA template and cDNA was produced after reverse transcription (RT) was completed (Nelsen *et al.,* 1999). For the first round of polymerase chain reaction (PCR), primers leader-p21 and Qi (Table 1) were used with the Expand Long PCR system (Boehringer Mannheim, Inc.). The second round PCR was completed similarly on a $10^{-3}$ dilution of the first round PCR products using 5′-382 and p75 (Table 1) as the primer pair. The PCR products were separated on a 1% agarose gel and each DNA band was purified by the use of a QIAgen gel purification kit.

## Molecular cloning and nucleotide sequencing

The purified RT-PCR fragments were cloned into pGEM-T vector (Promega) and resulting plasmids were screened for cDNA inserts using conventional methods (Sambrook *et al.,* 1989). Three to five plasmids were identified for each of four constructs and seven clones were sequenced (S-2, S-7a, S7b, I2-7, S-8, S-9a, S9b). Nucleotide sequencing was performed using the ABI 377 automatic sequencer in the Advanced Genetic Analysis Center, University of Minnesota, with the vector sequencing primers (T7 and SP6) or viral-specific primers (Table 1). The GCG package 10.0-UNIX (University of Wisconsin) and DNASTAR (Intelligenetics Inc.) were used to analyze the sequences.

## ACKNOWLEDGMENTS

The authors thank Dennis Foss, Daniel Mickelson, and Faith Klebs for their insightful discussions. Peter Plagemann, Kathleen Conklin, and Mark Rutherford are sincerely appreciated for their insightful comments. The work was supported by grants from PIC USA, the National Pork Producers Council, and Boehringer Ingelheim Vetmedica, Inc.

## REFERENCES

Allende, R., Lewis, T. L., Lu, Z., Rock, D. L., Kutish, G. F., Ali, A., Doster, A. R., and Osorio, F. A. (1999). North American and European porcine

reproductive and respiratory syndrome viruses differ in non-structural protein coding regions. *J. Gen. Virol.* **80,** 307–315.

Brian, D. A., and Spaan, W. J. M. (1997). Recombination and coronavirus defective interfering RNAs. *Semin. Virol.* **8,** 101–111.

Cavanagh, D., Brian, D. A., Enjuanes, L., Holmes, K. V., Lai, M. M., Laude, H., Siddell, S. G., Spaan, W., Taguchi, F., and Talbot, P. J. (1990). Recommendations of the Coronavirus Study Group for the nomenclature of the structural proteins, mRNAs, and genes of coronaviruses. *Virology* **176,** 306–307.

Chang, K.-Y., and Tinoco, I., Jr. (1994). Characterization of a "kissing" hairpin complex derived from the human immunodeficiency virus genome. *Proc. Natl. Acad. Sci. USA* **91,** 8705–8709.

Chang, R. Y., Hofmann, M. A., Sethna, P. B., and Brian, D. A. (1994). A cis-acting function for the coronavirus leader in defective-interfering RNA replication. *J. Virol.* **68,** 8223–8231.

Collins, J. E., Benfield, D. A., Christianson, W. T., Harris, L., Hennings, J. C., Shaw, D. P., Goyal, S. M., McCullough, S., Morrison, R. B., Joo, H. S., Gorcyca, D. E., and Chladek, D. W. (1992). Isolation of swine infertility and respiratory syndrome virus (isolate ATCC VR-2332) in North America and experimental reproduction of the disease in gnotobiotic pigs. *J. Vet. Diagn. Invest.* **4,** 117–126.

Cologna, R., and Hogue, B. G. (2000). Identification of a bovine coronavirus packaging signal. *J. Virol.* **74,** 580–583.

Conzelmann, K., Visser, N., van Woensel, P., and Thiel, H. (1993). Molecular characterization of porcine reproductive and respiratory syndrome virus, a member of the arterivirus group. *Virology* **193,** 329–339.

den Boon, J. A., Faaberg, K. S., Meulenberg, J. J., Wassenaar, A. L., Plagemann, P. G., Gorbalenya, A. E., and Snijder, E. J. (1995). Processing and evolution of the N-terminal region of the arterivirus replicase ORF1a protein: Identification of two papainlike cysteine proteases. *J. Virol.* **69,** 4500–4505.

Frohman, M. A. (1994). On beyond classic RACE (rapid amplification of cDNA ends). *PCR Methods Appl.* **4,** S40–S58.

Godeny, E. K., Chen, L., Kumar, S. N., Methven, S. L., Koonin, E. V., and Brinton, M. A. (1990). Complete genomic sequence and phylogenetic analysis of the lactate dehydrogenase-elevating virus (LDV). *Virology* **194,** 585–596.

Hofmann, M. A., Sethna, P. B., and Brian, D. A. (1990). Bovine coronavirus mRNA replication continues throughout persistent infection in cell culture. *J. Virol.* **64,** 4108–4112.

Huang, A. S. (1977). Viral pathogenesis and molecular biology. *Bacteriol. Rev.* **41,** 811–821.

Jia, W., Karaca, K., Parrish, C. R., and Naqi, S. A. (1995). A novel variant of avian infectious bronchitis virus resulting from recombination among three different strains. *Arch. Virol.* **140,** 259–271.

Keck, J. G., Matsushima, G. K., Makino, S., Fleming, J. O., Vannier, D. M., Stohlman, S. A., and Lai, M. M. C. (1988). In vivo RNA–RNA recombination of coronavirus in mouse brain. *J. Virol.* **62,** 1810–1813.

Keffaber, K. K. (1989). Reproductive failure of unknown etiology. *Am. Assoc. Swine Prac. Newsl.* **1,** 1–9.

Lai, M. M. C., Baric, R. S., Makino, S., Keck, J. G., Egbert, J., Leibowitz, J. L., and Stohlman, S. A. (1985). Recombination between nonsegmented RNA genomes of murine coronaviruses. *J. Virol.* **56,** 449–459.

Lai, M. M. (1992). RNA recombination between animal and plant viruses. *Microb. Rev.* **56,** 61–79.

Lai, M. M. C. (1996). Recombination in large RNA viruses: Coronaviruses. *Semin. Virol.* **7,** 381–388.

Li, K., Chen, Z., and Plagemann, P. (1999). High-frequency homologous genetic recombination of an arterivirus, lactatedehydrogenase-elevating virus, in mice and evolution of neuropathogenic variants. *Virology* **258,** 73–83.

Makino, S., Taguchi, F., and Fujiwara, K. (1984). Defective interfering particles of mouse hepatitis virus. *Virology* **133,** 9–17.

Makino, S., Fujioka, N., and Fujiwara, K. (1985). Structure of the intracellular defective viral RNAs of defective interfering particles of mouse hepatitis virus. *J. Virol.* **54,** 329–336.

Makino, S., Shieh, C.-K., Soe, L. H., Baker, S. C., and Lai, M. M. C. (1988). Primary structure and translation of a defective interfering RNA of murine coronavirus. *Virology* **166,** 550–560.

Makino, S., Yokomori, K., and Lai, M. M. (1990). Analysis of efficiently packaged defective interfering RNAs of murine coronavirus: Localization of a possible RNA-packaging signal. *J. Virol.* **64,** 6045–6053.

Masters, P. S., Koetzner, C. A., Kerr, C. A., and Heo, Y. (1994). Optimization of targeted RNA recombination and mapping of a novel nucleocapsid gene mutation in the coronavirus mouse hepatitis virus. *J. Virol.* **68,** 328–337.

Mendez, A., Smerdou, C., Izeta, A., Gebauer, F., and Enjuanes, L. (1996). Molecular characterization of transmissible gastroenteritis coronavirus defective interfering genomes: Packaging and heterogeneity. *Virology* **217,** 495–507.

Meng, X.-J., Paul, P. S., and Halbur, P. G. (1994). Molecular cloning and nucleotide sequences of the 3′-terminal genomic RNA of the porcine reproductive and respiratory syndrome virus. *J. Gen. Virol.* **75,** 1795–1801.

Meng, X. J., Paul, P. S., Morozov, I., and Halbur, P. G. (1996). A nested set of six or seven subgenomic mRNAs is formed in cells infected with different isolates of porcine reproductive and respiratory syndrome virus. *J. Gen. Virol.* **77,** 1265–1270.

Meulenberg, J. J. M., de Meijer, E. J., and Moormann, R. J. M. (1993a). Subgenomic RNAs of Lelystad virus contain a conserved leader–body junction sequence. *J. Gen. Virol.* **74,** 1697–1701.

Meulenberg, J. J. M., Hulst, M. M., de Meijer, E. J., Moonen, P. L. J. M., den Besten, A., de Kluyver, E. P., Wensvoort, G., and Moormann, R. J. M. (1993b). Lelystad virus, the causative agent of porcine epidemic abortion and respiratory syndrome (PEARS), is related to LDV and EAV. *Virology* **192,** 62–72.

Murtaugh, M. P., Elam, M. R., and Kakach, L. T. (1995). Comparison of the structural protein coding sequences of the VR-2332 and Lelystad virus strains of the PRRS virus. *Arch. Virol.* **140,** 1451–1460.

Nagy, P. D., and Simon, A. E. (1997). New insights into the mechanism of RNA recombination. *Virology* **235,** 1–9.

Nelsen, C. J., Murtaugh, M. P., and Faaberg, K. S. (1999). Porcine reproductive and respiratory syndrome virus comparison: Divergent evolution on two continents. *J. Virol.* **73,** 270–280.

Palmer, G. A., Kuo, L., Chen, Z., Faaberg, K. S., and Plagemann, P. G. W. (1995). Sequence of the genome of lactate dehydrogenase-elevating virus: Heterogenicity between strains P and C. *Virology* **209,** 637–642.

Penzes, Z., Tibbles, K., Shaw, K., Britton, P., Brown, T. D. K., and Cavanagh, D. (1994). Characterization of a replicating and packaged defective RNA of avian coronavirus infectious bronchitis virus. *Virology* **203,** 286–293.

Plagemann, P. G. W., and Moennig, B. (1992). Lactate dehydrogenase-elevating virus, equine arteritis virus and simian hemorrhagic fever virus: A new group of positive stranded RNA viruses. *Adv. Virus Res.* **41,** 99–192.

Rossow, K. D., Shivers, J. L., Yeske, P. E., Polson, D. D., Rowland, R. R., Lawson, S. R., Murtaugh, M. P., Nelson, E. A., and Collins, J. E. (1999). Porcine reproductive and respiratory syndrome virus infection in neonatal pigs characterized by marked neurovirulence. *Vet. Rec.* **144,** 444–448.

Sambrook, J., Fritsch, E. F., and Maniatis, T. (1989). Molecular Cloning. A Laboratory Manual, 2nd ed. Cold Spring Harbor Laboratory Press, Cold Spring Harbor, NY.

Snijder, E. J., den Boon, J. A., Horzinek, M. C., and Spaan, W. J. M. (1991). Characterization of defective interfering RNAs of Berne virus. *J. Gen. Virol.* **72,** 1635–1643.

Snijder, E. J., van Tol, H., Pedersen, K. W., Raamsman, M. J., and de Vries, A. A. (1999). Identification of a novel structural protein of arteriviruses. *J. Virol.* **73,** 6335–6345.

van der Most, R. G., Bredenbeek, P. J., and Spaan, W. J. M. (1991). A domain at the 3′ end of the polymerase gene is essential for encap-

sidation of coronavirus defective interfering RNAs. *J. Virol.* **65,** 3219–3226.

van Dinten, L. C., den Boon, J. A., Wassenaar, A. L., Spaan, W. J., and Snijder, E. J. (1997). An infectious arterivirus cDNA clone: Identification of a replicase point mutation that abolishes discontinuous mRNA transcription. *Proc. Natl. Acad. Sci. USA* **94,** 991–996.

van Marle, G., Dobbe, J. C., Gultyaev, A. P., Luytjes, W., Spaan, W. J., and Snijder, E. J. (1999). Arterivirus discontinuous mRNA transcription is guided by base pairing between sense and antisense transcription-regulating sequences. *Proc. Natl. Acad. Sci. USA* **96,** 12056–12061.

Wang, L., Junker, D., and Collison, E. W. (1993). Evidence of natural recombination within the S1 gene of the infectious bronchitis virus. *Virology* **192,** 710–716.

Wensvoort, G., Terpstra, C., Pol, J. M. A., ter Laak, E. A., Bloemraad, M., de Kluyver, E. P., Kragten, C., van Buiten, L., den Besten, A., Wagenaar, F., Broekhuijsen, J. M., Moonen, P. L. J. M., Zetstra, T., de Boer, E. A., Tibben, H. J., de Jong, M. F., van't Veld, P., Groenland, G. J. R., van Gennep, J. A., Voets, M. T., Verheijden, J. H. M., and Braamskamp, J. (1991). Mystery swine disease in the Netherlands: The isolation of Lelystad virus. *Vet. Q.* **13,** 121–130.

Yuan, S., Nelsen, C. J., Murtaugh, M. P., Schmitt, B. J., and Faaberg, K. S. (1999). Recombination between North American strains of porcine reproductive and respiratory syndrome virus. *Virus Res.* **61,** 87–98.